

Investigation of Seasonal Effects on Two-Stroke Marine Diesel Engine Performance Parameters and Emissions

Bulut Ozan Ceylan¹

Received: 26 October 2023 / Accepted: 13 December 2023
© Harbin Engineering University and Springer-Verlag GmbH Germany, part of Springer Nature 2023

Abstract

In comparison to onshore facilities, ships, and their machinery are subjected to challenging external influences such as rolling, vibration, and continually changing air & cooling water temperatures in the marine environment. However, these factors are typically neglected, or their consequences are deemed to have little effect on machinery, the environment, or human life. In this study, seasonal air & seawater temperature effects on marine diesel engine performance parameters and emissions are investigated by using a full-mission engine room simulator. A tanker ship two-stroke main engine MAN B&W 6S50 MC-C with a power output of 8 600 kW is employed during the simulation process. Furthermore, due to its diverse risks, the Marmara Region is chosen as the application area for real-time average temperature data. Based on the research findings, even minor variations in seasonal temperatures have a significant influence on certain key parameters of a ship's main engine including scavenge pressure, exhaust temperatures, compression and combustion pressures, fuel consumption, power, and NO_x-SO_x-CO_x emissions. For instance, during the winter season, the cylinder compression pressure (p_c) is recorded at 94 bar, while the maximum pressure (p_z) reaches 110 bar. In the summer, p_c experiences a decrease of 81 bar, while p_z is measured at 101 bar. The emission of nitrogen oxides (NO_x) exhibits a measurement of 784 parts per million (ppm) during winter and 744 in summer. The concentration of sulfur oxides (SO_x) is recorded at 46 ppm in winter and 53 in summer. Given the current state of global warming and climate change, it is an undeniable fact that the impact of these phenomena will inevitably escalate.

Keywords Marine environment; Air & seawater temperature; Shipping emissions; Marine diesel engine; Engine room simulator; Fuel consumption; Turkish Straits

1 Introduction

The function of shipping is crucial for guaranteeing the sustainability of global trade. Internal combustion engines are frequently chosen as the main propulsion force for ships in this industry (Noor et al., 2018; Ni et al., 2020). It is predicted that this type of engine is a component of

90–99% of currently operated vessels (Chybowski et al., 2015). In the internal combustion engine classification, diesel engines are the pioneer engine type in the maritime field (Tadros et al., 2020). Additionally, two and four-stroke marine-type diesel engines are used as the main power source of the propulsion force of the ships frequently (Ceylan, 2023). Therefore, it can be considered that marine diesel engines are the most important components of ships (Guo et al., 2018). On the other side, two-stroke marine diesel engines are used as the main engine in a wide range of commercial ships (Ryu et al., 2016; Yang et al., 2020; Ramsay et al., 2023). Since, two-stroke marine diesel engines have higher efficiency and lower specific fuel consumption (SFC) than the other types of internal combustion engines (Llamas & Eriksson, 2019; Vera-García et al., 2020). Furthermore, these types of engines have been designed and manufactured in large sizes, high power, and complex structures with numerous systems (Ceylan et al., 2021). The fundamental engine components and cross-section of a two-stroke marine-type diesel engine are demonstrated in Figure 1 (MAN, 2023).

The marine engine is an essential component of a vessel

Article Highlights

- Seasonal air & seawater temperature effects on two-stroke marine diesel engine performance were investigated in this study.
- Measurements were taken from a 183-meter product tanker ship equipped with a MAN B&W 6S50 MC-C main engine.
- According to the findings, minor seasonal temperature variations have a significant impact on atmospheric pollution.
- The main engine scavenge pressure, exhaust temperatures, compression and combustion pressures, NO_x-SO_x-CO_x emissions, and fuel consumption were critically affected.

✉ Bulut Ozan Ceylan
bceylan@bandirma.edu.tr

¹ Department of Maritime Transportation and Management Engineering, Bandirma Onyedü Eylül University, Bandirma 10200, Balikesir, Turkey

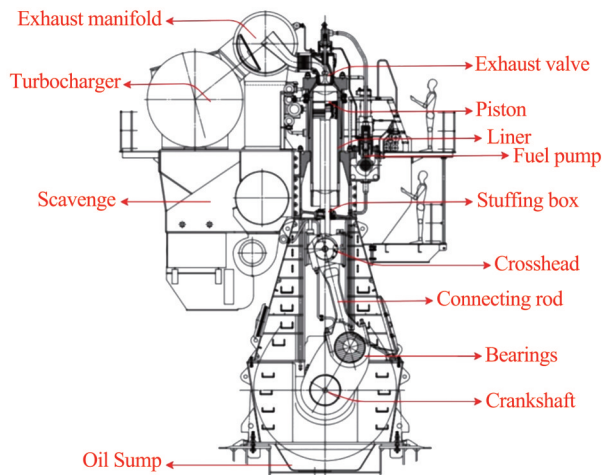


Figure 1 Two-stroke marine-type diesel engine cross-section

as it serves as the major power source while also being a significant contributor to pollution through the combustion of various fuel types, enabling the conversion of energy into mechanical force (Tadros et al., 2023). During commercial operations, ships with higher-capacity diesel engines produce a substantial quantity of exhaust gases. These shipping-related airborne emissions lead to pollution in the atmosphere. The main emissions that exhaust gases may emit into the environment are sulfur oxides- SO_x , nitrogen oxides- NO_x , carbon monoxide-CO, carbon dioxide- CO_2 , particulate matter-PM, volatile organic compounds-VOCs, black carbon-BC, organic carbon-OC. (Welaya et al., 2013; Nahim et al., 2015; Wang et al., 2017; Zincir & Arslanoglu, 2024). According to the International Maritime Organization (IMO), the international shipping industry is responsible for 2%–3% of global CO_2 , 10%–15% of NO_x , and 4%–5% of SO_x emissions (Buhaug et al., 2009; Gaspar et al., 2015). Transportation-related exhaust emissions are the primary pollutant source and contribute to health problems and ecological effects such as global warming, climate change, acidification, eutrophication, and deterioration of air quality (Zetterdahl et al., 2017; Bilgili & Buğra Çelebi, 2021; Mocerino et al., 2021). To transition towards a more environmentally sustainable future, it is imperative to mitigate the adverse impacts of ships on the natural environment through measures aimed at enhancing operational efficiency and minimizing ship emissions (Karatuğ et al., 2023; Kanberoğlu et al., 2023). Alongside the environmental considerations, the economic implications of reducing fuel consumption are of paramount importance within the realm of maritime transportation (Yuksel et al., 2023).

There are different studies about air temperature effects on diesel engine parameters in the literature. Torregrosa et al (2006) tested the impact of charge air and cooling temperature on diesel engine performance parameters and emissions. The test engine is a single-cylindered common rail system diesel engine with a 76 mm bore and 87 mm

stroke length. Banugopan et al (2010) carried out an investigation on ethanol-fueled diesel engine with varying inlet air temperatures. The used engine is a single-cylinder with a bore of 88 mm, a stroke of 110 mm, and 5.9 kW at 1 800 r/min. Kumar & Raj (2013) researched how the timing of fuel injection and the temperature of the intake air affected the combustion and emission characteristics of a dual-fuel diesel engine. Tests are carried out by using a small four-stroke, single-cylindered, air-cooled diesel engine with a bore of 78 mm, and a stroke of 68 mm. Pan et al. (2015) investigated the impact of air temperature on dual-fuel methanol diesel engine performance and emissions. They used a 6-cylinder turbocharged inter-cooled engine with 126 mm bore, 130 mm stroke, and 247 kW power at 1 900 r/min. Sarjoavaara et al (2015) investigated the effect of a charge air temperature on a dual-fuel diesel engine with 120 kW at 2 300 r/min. Woo et al (2016) analyzed the impact of charge air temperature and common rail pressure on ethanol-fueled single-cylinder light-duty diesel engine with 83 mm bore and 92 mm stroke. Wu et al (2017) experimented with different intake air temperatures and EGR ratios to get the best performance and emissions from a diesel hydrogen gas engine. They used a small diesel engine with a 94 mm bore, 90 mm stroke, and 9.2 kW power at 2 400 r/min. The aforementioned studies have examined the effects of charge air temperature on the performance parameters of diesel engines. However, there is a lack of thorough research specifically focused on 2-stroke, large-sized marine diesel engines. Additionally, no research has been identified that investigates the impact on ship machinery using real air & seawater temperature averages in a particular region as a reference.

Commercial ships navigate several maritime regions, thereby exposing them to a diverse range of ambient and seawater temperatures. Nevertheless, conducting research to investigate the impact of varying temperatures on ship engines in a real engine room environment is a challenging problem owing to factors such as seasonal variations and geographical differences. On the other side, performing empirical research on the main engines, which are essential components of the ship and engine room, entails significant potential risks. Testing the effects of oil filter contamination on a real ship's main engine, for example, is highly perilous since it might result in severe equipment malfunction (Ceylan et al., 2022a). In this light, conducting such investigations in a simulation environment is relatively safe for property, the environment, and human life (Dere & Deniz, 2019). Moreover, when compared with the real scenario, it is very simple to maintain the constancy of all variables inside the simulation setting, except for the parameter under investigation. Consequently, focusing on altering a single element and analyzing its impact on the machinery appears to be a more reliable approach. For this reason, several critical investigations are being conducted

with the use of ship engine simulators (Dimitrios, 2012; Kocak & Durmusoglu, 2018; Yutuc, 2020; Knežević et al., 2020; Chybowski et al, 2020; Stanivuk et al., 2021; Ceylan et al 2022b).

In this study, seasonal air & seawater temperature effects on two-stroke marine-type diesel engine performance parameters and airborne emissions are investigated with the help of full-mission ERS. In the simulation process, measurements are taken from a 183-meter product tanker ship equipped with a MAN B&W 6S50 MC-C main engine. Within this scope, the paper is organized as follows. This chapter gives the motivation behind the research. Section 2 introduces the material and method of the study including state of knowledge, engine room simulator, expert profiles, input parameters sampling, and methodology of the study. Section 3 includes a full mission simulator application. A discussion of the study is in section 4. Finally, section 5 concludes the research and advises future studies.

2 Material and method

This section offers a brief overview of the used state of knowledge, engine room simulator, expert profiles, sampling parameters, and methodology of the study.

2.1 State of the Knowledge

In this study, the internal combustion marine diesel engine is investigated using the full-mission ERS. Air & seawater temperature effects on the diesel engine performance parameters are investigated in the simulation process. During the simulation, various parameters such as combustion pressure, cylinder power, and fuel oil consumption are recorded and analyzed. The power of mechanical losses should be estimated as the difference between measured and effective power as shown in Eq. 1.

$$P_{ml} = P_i - P_e \tag{1}$$

Here P_{ml} (kW) indicates the power of mechanical losses, P_i (kW) is the measured power, and P_e (kW) is the measured effective power.

Eq. 2 is used to calculate the mechanical efficiency:

$$\eta_m = \frac{P_e}{P_i} \times 100 \tag{2}$$

where η_m is the mechanical efficiency of the engine (%).

Eq. 3. is used to get the indicated engine efficiency:

$$\eta_i = \frac{P_i}{\dot{m}_f H_i} \times 3\,600 \times 100 \tag{3}$$

where η_i is engine indicated efficiency, \dot{m}_f (kg/h) is fuel

mass flow and H_i (kJ/kg) is lower heating value of the fuel.

Eq. 4. is used to get the effective engine efficiency:

$$\eta_e = \frac{P_e}{\dot{m}_f H_i} \times 3\,600 \times 100 \tag{4}$$

where η_e is engine effective efficiency.

An Eq. 5. is used to determine the engine’s mean effective pressure:

$$p_e = \frac{P_e \times \tau}{2 \times z \times n V_o} \times \frac{6}{10} \tag{5}$$

where p_e is engine mean effective pressure, τ engine stroke (in this study $\tau=2$ because a 2-stroke marine type diesel engine is used in the simulation), z is the number of engine cylinders (in this study $z=6$ because MAN B&W 6S50 MC-C engine is used in the simulation), n (r/min) is measured engine revolution speed per minute (in this study $n=105$), V_o (m³) is per engine cylinder operating volume.

The operating volume of one engine cylinder is calculated in Eq. 6:

$$V_o = \frac{D^2 \times \pi}{4} \times s \tag{6}$$

where D (m) is the cylinder bore and s (m) is the stroke of the engine cylinder.

An Eq. 7. is used to calculate the engine’s effective torque:

$$M_e = \frac{P_e}{2 \times \pi \times n} \times 60\,000 \tag{7}$$

Finally, specific effective fuel consumption (SFC_e) is calculated by Eq. 8:

$$SFC_e = \frac{\dot{m}_f \times 1\,000}{P_e} \tag{8}$$

where SFC_e (g/kWh) is the engine’s specific effective fuel consumption (Mrzljak et al., 2017; Monieta, 2021; ISO, 2022).

2.2 Engine room simulator

Engine room simulators (ERS) play a crucial role in maritime education and academic research due to their ability to mitigate the risks associated with practical training on actual ships. Moreover, modern simulators have been expertly designed to accurately emulate the functionality of real engines, hence yielding highly realistic outcomes (Wärtsilä-Transas, 2023). On the other hand, ERS 5 000 has been specifically designed for the training; covers maritime training compliance with the STCW requirements; meets the requirements of International Maritime Organi-

zation (IMO) conventions and International Electrotechnical Commission (IEC) standards, and is approved by Det Norske Veritas (DNV) (Kongsberg Maritime, 2022; Wärtsilä-Transas, 2023). Due to this rationale, there has been a significant surge in the utilization of simulators in recent years.

In this study, the main engine parameters are investigated in Transas 5 000 ERS by using the simulator's malfunction interface. During the simulation process, the engine is operated at 105 r/min under the bridge command of full ahead. As the main engine, MAN B&W 6S50 MC-C engine, two strokes, single-acting, direct reversible, crosshead type marine diesel engine with 6 cylinders (500 mm bore and 2 000 mm stroke length) is selected. The main engine generates a maximum of 8 600 kW at 127 r/min. Technical descriptions of the engine are demonstrated in Table 1. According to this engine type, engine commands and r/min set points are shown in Table 2.

Table 1 Technical specifications of the simulator

Ship type	Oil/Chemical product tanker
Dead weight (t)	50 000
Length (m)	183
Breath (m)	32.2
Max. speed (kn)	15.7
Max. continuous power	8 600 kW at 127 r/min
Main engine type	MAN B&W model 6S50 MC-C
Number of cylinders	6
Cylinder bore (mm)	500
Stroke length (mm)	2 000

Table 2 Technical description of the engine commands

Engine command	Revolution (r/min)
Navigation full ahead	89/128
Full ahead	76/80
Half ahead	68/71
Slow ahead	56/58
Dead slow ahead	32/43
Stop	0
Dead slow astern	-38
Slow astern	-58
Half astern	-75
Full astern	-85/90

2.3 Expert profiles

The methodology of the investigation encompasses two essential components. The first step entails designing a simulation environment that closely resembles the real sce-

nario in order to achieve accurate results. This is followed by the second stage of analyzing the data that is generated. According to the methodological approach of the study, expert knowledge is utilized in the realistic simulation design and the analysis of the output data. An expert group of the study that is shown in Table 3 consists of experienced seafarers who have worked on various types of ships as an oceangoing engineer.

Table 3 Expert profiles of the study

Expert code	Ship experience	Current position
E.1	Oceangoing chief engineer	University-academician
E.2	Oceangoing chief engineer	Shipping company-oceangoing chief engineer
E.3	Oceangoing chief engineer	Shipping company-oceangoing chief engineer
E.4	Oceangoing second engineer	Port state control-port state control officer
E.5	Oceangoing second engineer	university-academician
E.6	Oceangoing second engineer	Shipping company-oceangoing second engineer

2.4 A sampling of input parameters

The Turkish Straits, which divide Asia and Europe, have a length of 164 nautical miles (Kaptan et al., 2020). The three-part Turkish Straits System comprises the Istanbul Strait, the Sea of Marmara, and the Canakkale Strait (Tonoğlu et al., 2022). The Marmara region, characterized by its dense population and significant maritime activity, is selected as the focal location for investigation. Additionally, this region has two critical narrow waterways, such as the Bosphorus and the Dardanelles, and these waterways have meteorological and oceanographical threats such as current regimes, low visibility, and winds (Arslan & Turan, 2009; Tonoğlu et al., 2022). Hence, the possible ramifications of ship machinery malfunctions in the chosen destination might be catastrophic, affecting property, the environment, and human lives. Furthermore, the region's extensive ship traffic contributes to a range of emissions such as CO, CO₂, NO_x, SO_x and PM (Lamas et al., 2013; Toscano et al., 2021; Ay et al., 2022). As a result, the Marmara Region, which has diverse risks, is chosen as the application area for this study. The selected location is shown in Figure 2 (Google Earth, 2022).

The air temperature data used for the application is obtained from the monthly average temperatures recorded in the Marmara Region from 2021 (MGM, 2022a). Similarly, seawater temperature is obtained by taking the monthly average temperatures for the year 2021 (MGM, 2022b). The average air & seawater temperatures are shown in Table 4.

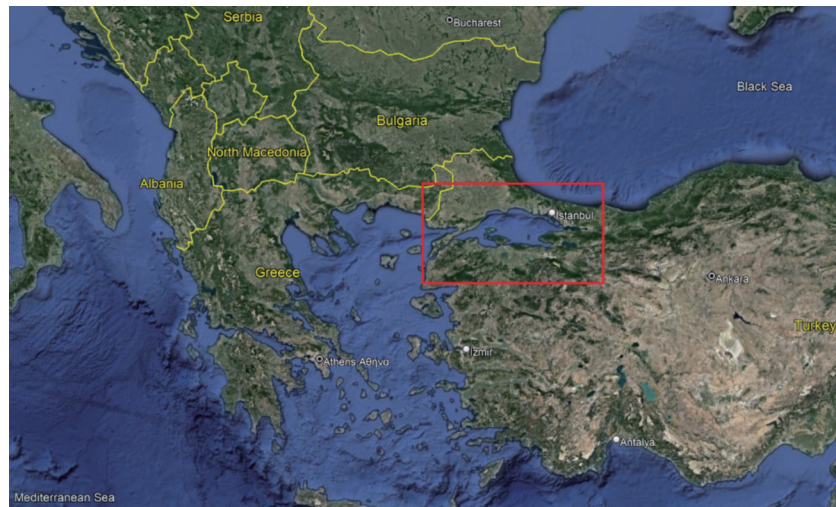


Figure 2 Selected application area of the study

These temperatures are separated into four seasons, averaged, and converted into four different input data sets. Accordingly, the first dataset has an air temperature of 8.4 °C and a seawater temperature of 11.7 °C. The second part has an average of 12.4 air and 13.0 °C seawater temperature. The third zone has an air temperature of 24.3 °C while the seawater average temperature of 23.8 °C. Finally, the fourth part consists of an air temperature of 16 °C and a seawater temperature of 18.7 °C.

Table 4 The average air and seawater temperature

Months of 2021	Average air temp. (°C)	Average seasonal air temp. (°C)	Average seawater temp. (°C)	Average seasonal seawater temp. (°C)
12	9.3		13.1	
1	8.2	8.4	11.6	11.7
2	7.7		10.4	
3	7.2		10.6	
4	11.8	12.4	12.0	13.0
5	18.3		16.5	
6	21.2		21.1	
7	25.8	24.3	25.0	23.8
8	25.9		25.4	
9	20.3		22.6	
10	15.0	16	18.4	18.7
11	12.8		15.2	

2.5 Methodology

Engine room simulator environments provide researchers with a viable option for undertaking realistic digital operations and tests. However, there is no standard procedure in this approach as the implementation of ERS in academic

studies is determined by the authors’ decision. Recent years have seen the development of an approach for using engine simulators as an academic tool to fill this need. According to this approach, the construction of a realistic simulation environment is the key element of the engine room simulation-based academic investigation methodology (Ceylan et al 2022b). Therefore, this study uses a modified realistic simulation design concept. The study’s methodological approach consists of three main steps. The average air & seawater temperatures of the Marmara Region, which is densely populated and has narrow waterways, are separated into four seasons. The obtained air & seawater temperatures are used as the input data sets of the method. After the input data is available, a realistic simulation environment is designed for the application. In this framework, the knowledge of 6 marine engineers who have a minimum oceangoing second engineer competency is used. Once the main engine is prepared, the simulation is started and the output data are recorded. Finally, these output data are analyzed with the help of the experts. The methodological framework of the study is illustrated in Figure 3.

3 Application

Investigation of seasonal air & seawater temperature effects on two-stroke marine diesel engine performance parameters are tested in Transas 5 000 ERS by using the simulator’s malfunction and main engine operator interface. The main engine used on the simulator is the 2-stroke MAN B&W 6S50 MC-C, which is frequently used in today’s commercial ships. Furthermore, this type of engine has been used in several academic investigations (Kökkülünk et al., 2016; Knežević et al, 2020; Monieta, 2021). During the simulation process, the engine is operated at 105 r/min under the bridge command of full ahead, the approximate

engine fuel load is %65, and the engine room ambient has 60% air humidity. Wärtsilä -Transas MAN B&W 6S50 MC-C main engine simulation interface is demonstrated in Figure 4 (Wärtsilä -Transas, 2023). The application is designed to categorize the input sets into 4 distinct seasons depending on the months. The months of December, January, and February are recognized to be part of the winter season.

The months of March, April, and May are considered to be part of the spring season. The months of June, July, and August are regarded to be members of the summer season. The months of September, October, and November are generally recognized as part of the autumn season. Data on the average temperature of seawater & air are recorded during these four months.

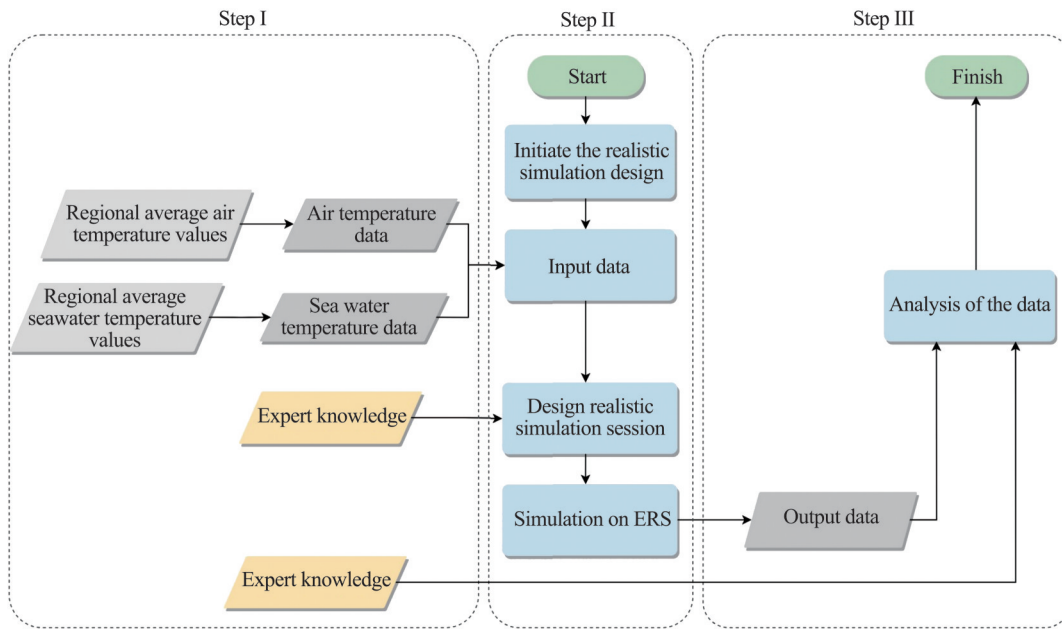


Figure 3 The methodological framework of the study

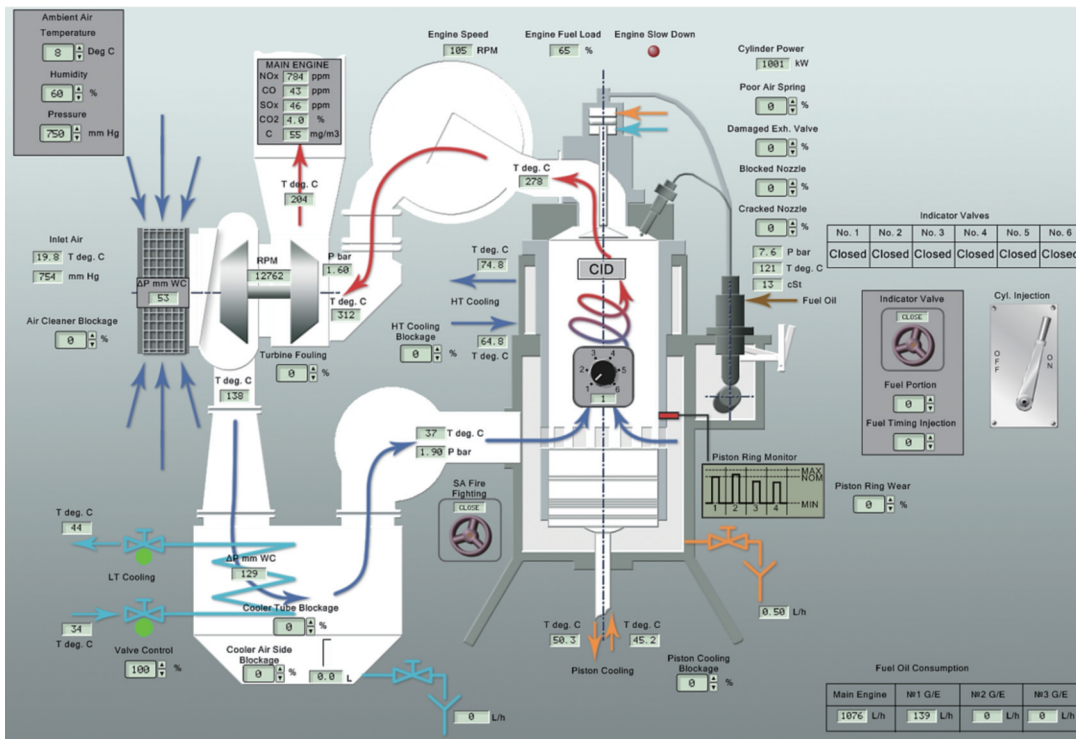


Figure 4 MAN B&W 6S50 MC-C simulation interface

The realistic simulation process is initiated and the input data are integrated into the simulator for 4 different seasons, according to the study’s methodological approach. Average air temperature of 8.4 °C and seawater temperature of 11.7 °C for the winter season, an average of 12.4 °C air and 13.0 °C seawater temperature for spring, 24.3 °C air and 23.8 °C seawater temperature for summer and autumn, air temperature of 16 °C and seawater temperature of 18.7 °C data are used in this framework. With the help of the experts, a realistic simulation environment is designed employing the collected data, and the session starts. All other variables are held constant during the measurement except for temperatures of ambient & seawater. Main engine operating parameters are recorded according to the average temperature values of each season. Table 5 presents the engine parameters that emerge at various seasonal temperatures.

The investigation is conducted on three distinct consoles, each utilizing the same scenario to simplify monitoring and consistent data comparison. Ambient air & seawater temperatures are altered, waited for the stabilization of engine parameters, and then the output data is recorded. For the winter season, the average effective pressure (p_e) of the main engine is measured as 15.3 bar, compression pressure (p_c) 94 bar, the maximum pressure (p_z) 110 bar, and timing angle (ϕ_{pz}) 9°, ignition angle (ϕ_{ign}) 1°. The winter season cylinder combustion graph is shown in Figure 5(a).

The average effective pressure (p_e) of the main engine is recorded at 15.4 bar during the spring season, with compression pressure (p_c) of 90 bar, the maximum pressure (p_z) of 108 bar, timing angle (ϕ_{pz}) of 10°, ignition angle (ϕ_{ign}) of 1°. Figure 5(b) depicts the corresponding cylinder combustion graph.

Table 5 Simulation results of the study

Engine parameters	Months			
	12-1-2	3-4-5	6-7-8	9-10-11
Average air temperature (°C)	8.4	12.4	24.3	16
Average seawater temperature (°C)	11.7	13.0	23.8	18.7
Engine air inlet temperature (°C)	19.8	24.3	36	28.1
Scavenge air temperature (°C)	138	139	141	139
LT cooling water scavenge inlet (°C)	34	37	37	36
LT cooling water scavenge outlet (°C)	44	45	45	44
Scavenge air temperature after cooler (°C)	37	37	37	36
Scavenge air pressure (bar)	1.9	1.7	1.5	1.6
HT cooling water cylinder inlet (°C)	64.8	64.7	65	65.1
HT cooling water cylinder outlet (°C)	74.8	74.7	75.1	75.1
Piston cooling oil inlet (°C)	45.2	45.3	45.2	45.2
Piston cooling oil outlet (°C)	50.3	50.7	50.6	50.5
Cylinder exhaust outlet temperature (°C)	278	293	333	305
TC exhaust inlet temperature (°C)	312	325	360	336
Exhaust manifold pressure (bar)	1.6	1.5	1.3	1.4
TC exhaust outlet temperature (°C)	204	221	264	235
TC (r/min)	12 762	12 420	11 705	12 140
NO _x emission (ppm)	784	771	744	760
CO emission (ppm)	43	41	39	40
SO _x emission (ppm)	46	48	53	49
CO ₂ emission (%)	4.0	4.2	4.7	4.4
C emission (mg/m ³)	55	55	57	56
p_e (bar)	15.3	15.4	15.3	15.3
p_z (bar)	110	108	101	105
p_c (bar)	94	90	81	86
Φ_{pz} (°)	9	10	11	10
Φ_{ign} (°)	1	1	1	1
Engine speed (r/min)	105	105	105	105
M/E F/O consumption (L/h)	1 076	1 081	1 082	1 079
Cylinder power (kW)	998	997	997	996

For the summer, the average effective pressure (p_e) of the main engine is measured as 15.3 bar, compression pressure (p_c) 81 bar, the maximum pressure (p_z) 101 bar, and timing angle (ϕ_{pz}) 11°, ignition angle (ϕ_{ign}) 1°. The summer season cylinder combustion graph is shown in Figure 5 (c).

For the autumn, the average effective pressure (p_e) of the main engine is measured as 15.3 bar, compression pressure (p_c) 86 bar, the maximum pressure (p_z) 105 bar, and timing angle (ϕ_{pz}) 11°, ignition angle (ϕ_{ign}) 1°. The autumn season cylinder combustion graph is shown in Figure 5 (d).

The output data is evaluated by experts under the study’s methodological framework. According to the findings, changes in air and sea temperature influence several variables, including scavenge-exhaust temperatures, emission values, and fuel consumption, along with the compression and combustion processes. The subsequent section will provide a discussion of these changes.

4 Discussion

Obtained simulation outputs are assessed using expert judgment under the methodology of the study. Air & seawater

temperature fluctuations’ effects on the ship’s main engine parameters are evaluated by a team of specialists comprised of marine engineers with academic and professional backgrounds. The lowest seawater & air temperature values are recorded in the Marmara Region during the winter season. The temperature difference between seawater & air is considerable. Both temperatures in the spring season are similar, hovering around 13 °C. Summer is characterized by exceptionally high temperatures and similar mean values. Eventually, autumn temperatures exhibit average values, with a substantial variation between them.

Ship engine rooms are restricted areas where different equipment such as boilers, separators, generators, compressors, and main engines work together in a complex structure. Even though fresh air is constantly taken from the outside of the ship and sent to the engine room through massive engine room fans, the temperature of the area is raised by fuel tanks, steam tracing pipes, and constantly operating machinery. For this reason, experimental evidence indicates that the air temperature entering the main engine is typically around 10 degrees Celsius greater than the seasonal average air temperature. Furthermore, the turbocharger (TC) provides air compression in the engine room by use of its compressor blades. A scavenge cooler is

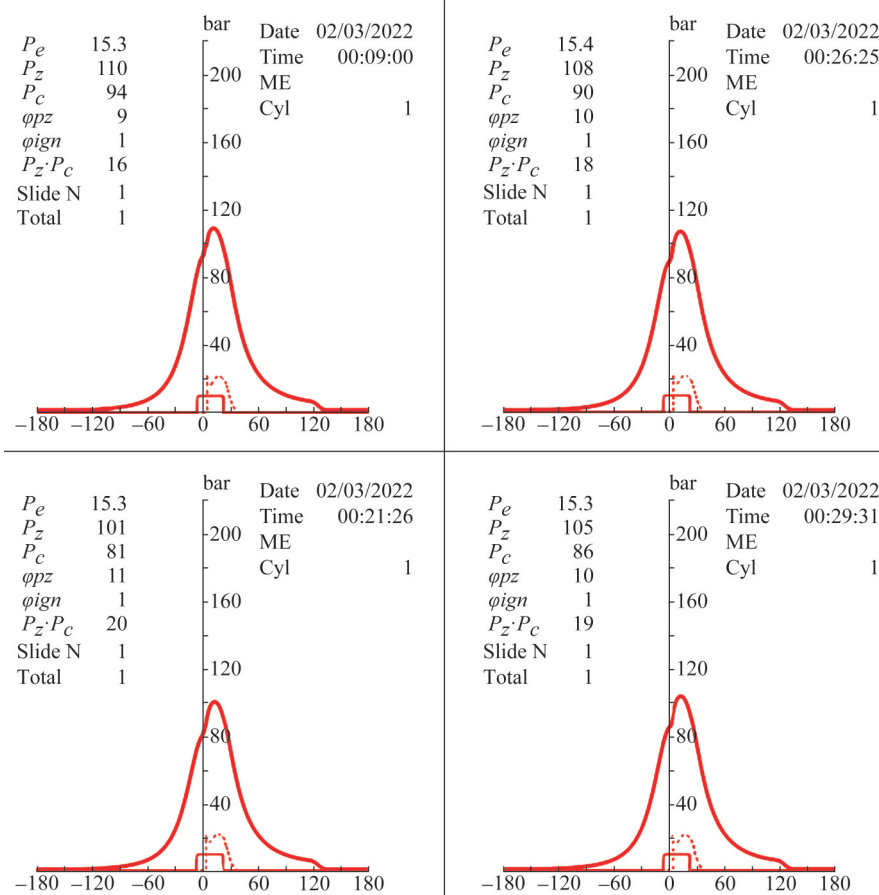


Figure 5 Seasonal cylinder combustion pressure graphs

employed to absorb excessive heat from the air caused by increased pressure.

In light of the simulation outputs, the scavenge air temperature of the main engine and the inlet & outlet of the LT cooling water are relatively unaffected by the seasonal temperature changes. Nevertheless, the speed of the TC, which is affected by the temperatures of the cylinder exhaust outlet and the pressure in the exhaust manifold, fluctuates throughout the year. Changing TC speed, on the other hand, affects the pressure of the compressed air. The scavenge air pressure, which is 1.9 in winter, decreases to 1.5 bar in summer. Exhaust manifold pressure also follows a similar trend with the highest value of 1.6 in winter and decreasing to 1.3 bar in summer. On the other hand, the inlet & outlet temperatures of the cylinder jacket cooling water and piston cooling oil are not affected much by the seasonal difference. No 1 seasonal graphs of the engine parameters are given in Figure 6.

The temperature of the cylinder exhaust outlet is a critical engine control system parameter. Seasonally, the exhaust outlet temperature drops from 333 °C in summer to 278 °C in winter as a result of the decrease in ambient air temperature. The studied engine has six cylinders and the exhaust temperature increases by about 30 °C since the exhaust gas from each cylinder is compressed in the exhaust manifold. The exhaust temperature difference between the cylinder exhaust outlet and the TC inlet is therefore recorded

differently. The temperature difference at the TC inlet and outlet is due to the conversion of the heat energy in the exhaust into motion energy.

When the emission values of the main engine are investigated, NO_x emission peaks at the highest value of 784 ppm, while it reaches the lowest value of 744 in summer. Despite the high temperature of the exhaust in the summer, the lower combustion pressures reduce NO_x formation. There is no significant difference in C emission. SO_x emission, on the other hand, has the lowest value at 46 ppm in winter and the highest value at 53 ppm in summer. This is due to high fuel consumption in the summer. CO emissions, on the other side, follow a similar pattern to NO_x emissions, peaking at 43 ppm in winter and dropping to 39 ppm in summer.

The efficiency of the engine is also significantly affected by changes in compression and combustion pressures of the cylinder. Considering the seasonal fuel consumption of the main engine, it is seen that 1 076 liters per hour in winter and 1 082 liters in summer. This scenario coincides with alterations in scavenge, compression, and combustion pressures. No 2 seasonal variation graphs of the engine values are given in Figure 7.

The engine is kept at full speed at 105 r/min under the full ahead bridge command throughout the simulation. Additionally, there is no significant change in Φ_{pz} and Φ_{ign} angles. However, the combustion pressure is directly

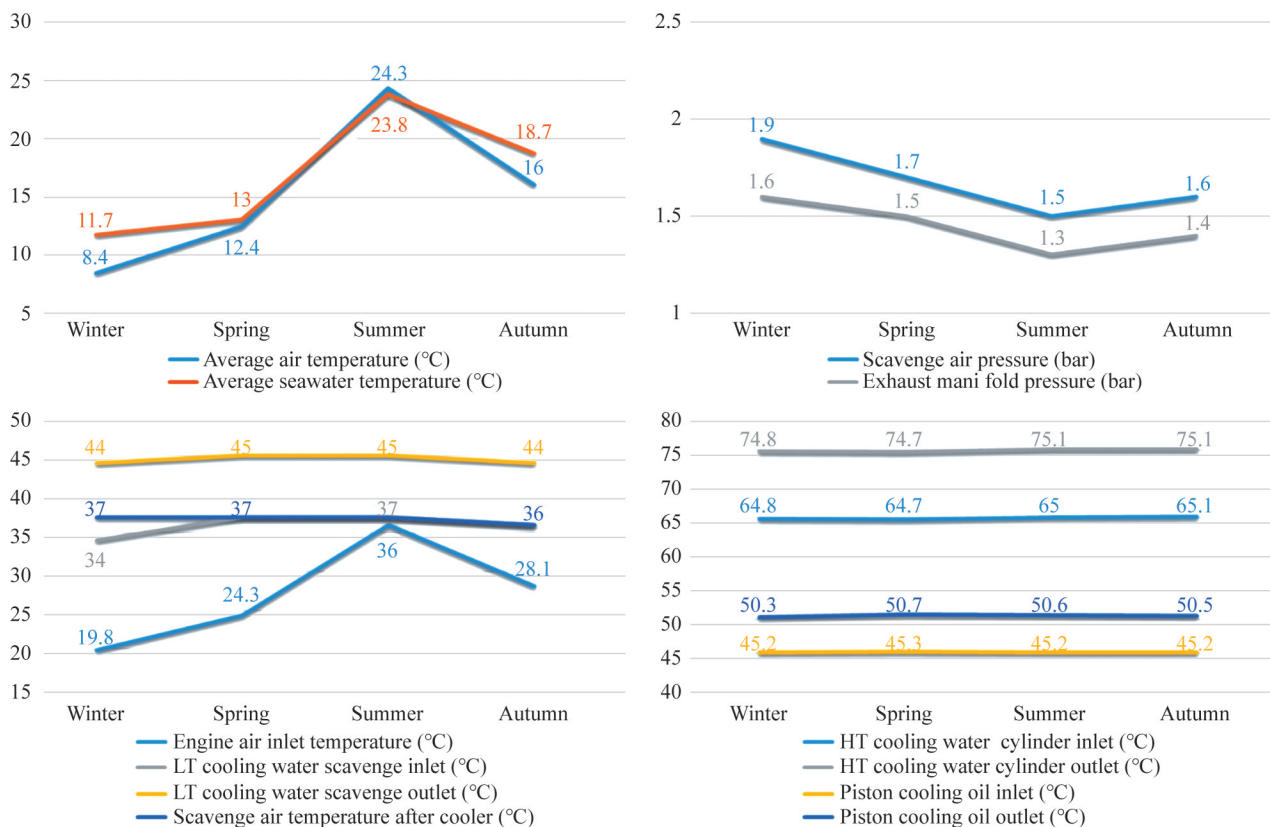


Figure 6 Seasonal variations of the engine parameters No 1

affected by the compression pressure in the cylinders. The p_c value is the highest at 94 bar in winter and the lowest value at 81 bar in summer. Similarly, the p_z value is recorded as 110 bar in winter and 101 bar in summer. The 0.4 bar difference in scavenge pressure between summer and winter results in a p_c and p_z difference of approximately 10 bar. The open and closed indicator diagrams below depict the seasons using specific colors: orange for summer, green for

for autumn, blue for spring, and red for winter. The cylinder p - V diagrams are shown in Figure 8.

The main engine cylinder p - Φ diagram is demonstrated in Figure 9. The enclosed graphic exhibits its maximum size during winter and the smallest area during summer. Based on these diagrams, it is evident that variations in temperature throughout the seasons affect the compression and combustion process of the engine.

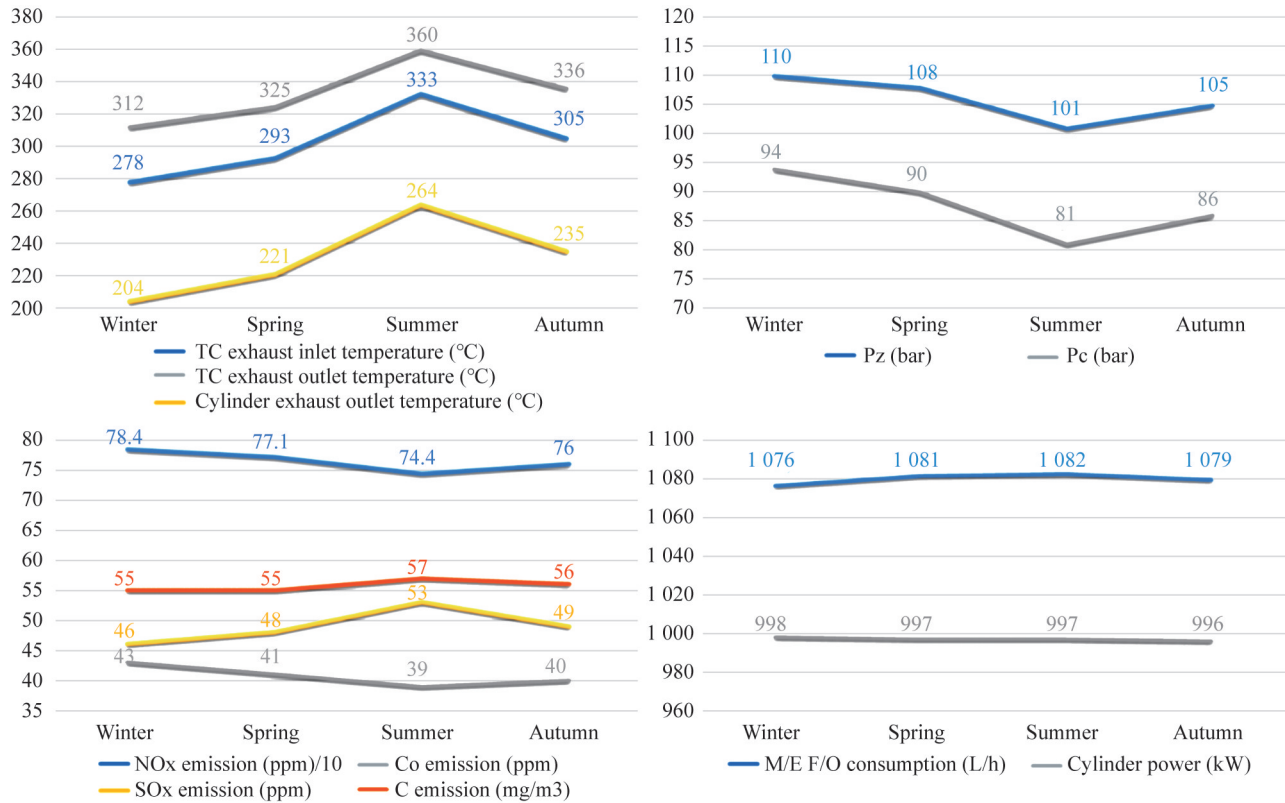


Figure 7 Seasonal variations of the engine parameters No 2

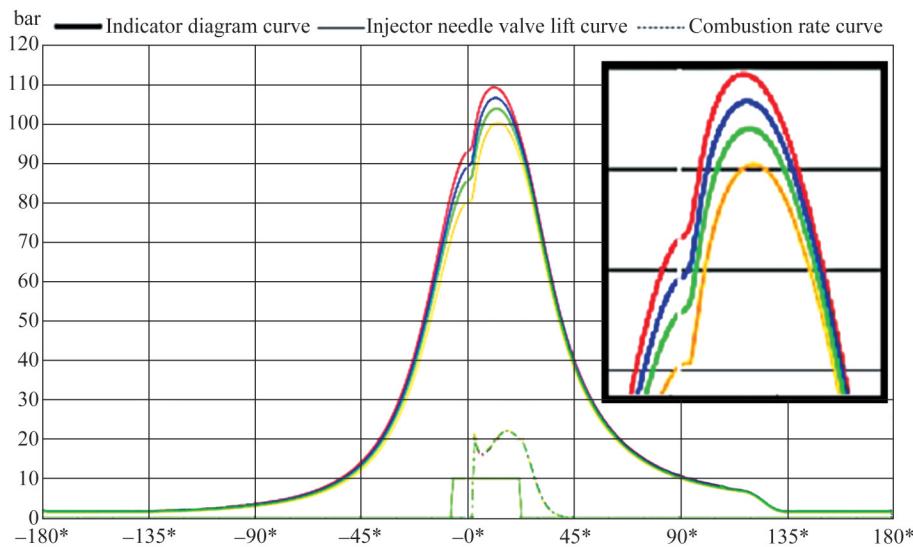


Figure 8 Cylinder p - V diagrams

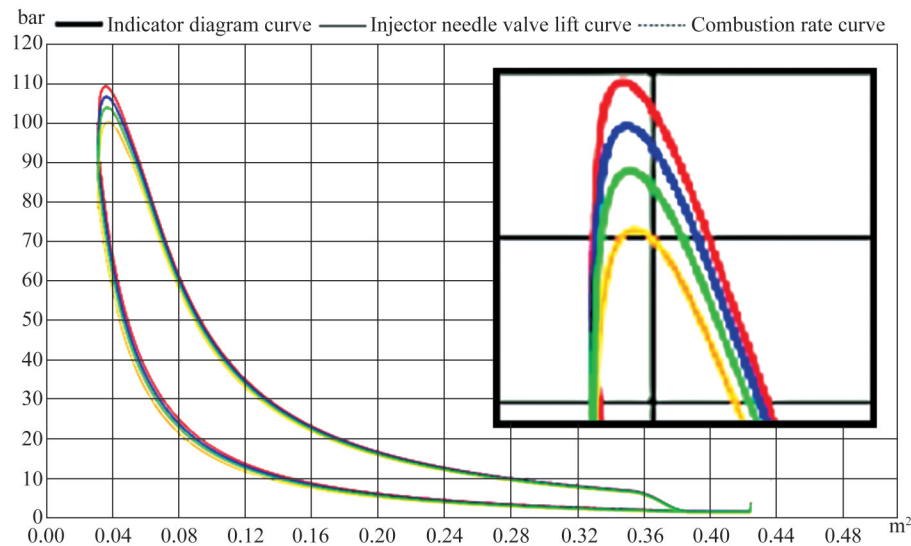


Figure 9 Cylinder p - Φ diagrams

5 Conclusion

Commercial ships, with their massive, complicated, and dynamic engineering structures, are constantly navigating throughout the world's oceans. Hence, the main engine, which is the driving force and most critical component of the ship, is subjected to a range of seasonal temperatures during its voyages. Even though commercial ships are constantly subjected to this variety of temperatures, the maritime industry lacks situational awareness regarding the consequences of this situation. In this line, this study aims to examine the effects of seasonal ambient air & seawater temperature variations on the main engine. To achieve this, a comprehensive investigation is conducted within a full mission engine room simulator, employing a realistic simulation design technique. The Marmara Region, characterized by high levels of maritime activity and the presence of two narrow sea passages, mainly the Dardanelles and Istanbul Straits, is chosen for one-year temperature data. Based on the results, fluctuations in seasonal temperatures have a notable impact on many parameters of the ship's main engine.

The main engine jacket and lubricating oil temperatures, which are secondary cooling systems that are not influenced by ambient air & seawater temperatures, did not demonstrate noteworthy fluctuations. Additionally, the simulated tanker ship operates at full head with an engine speed of 105 r/min. Therefore, the engine speed and the generated kW value are maintained constant by the control system.

Comparing the winter and summer seasons as regards the highest temperature differences, it is noted that the scavenge air temperature increased from 138 to 141 °C. Although there are no significant variations in the LT temperatures, the scavenge pressure decreases from 1.9 to 1.5 bar.

The observed decline in scavenge pressure can be related to a reduction in turbine speed, which decreases from 12 762 to 11 705 r/min. The temperatures at the cylinder exhaust outlet are recorded as 278 °C during the winter and 333 °C during the summer. Additionally, the exhaust manifold pressure is measured at 1.6 bar for winter and 1.3 bar for summer, resulting in a reduction in turbocharger speed during the summer season.

The change in scavenge pressure and temperature directly influenced the combustion process, leading to a decrease in p_c from 94 to 81 bar. With a decline in compression pressure, the value of p_z also drops from 110 to 101 bar. Consequently, the affected combustion process increases the main engine fuel consumption from 1 076 L/h in winter to 1 082 L/h in summer. In this case, the ship's main engine consumes an additional 6 L of fuel for every hour of operation during the summer. Furthermore, emissions of CO₂ increase from 4% to 4.7%, emissions of SO_x from 46 to 53 ppm, and emissions of C from 55 to 57 mg/m³. The NO_x value, which varies with the maximum combustion pressure (110 bar in winter and 101 bar in summer), decreases from 784 ppm to 744 ppm.

The results illustrate the possible effects of minor temperature variations on the combustion characteristics, fuel efficiency, and emissions of the ship's main engine quantitatively. While the literature on ship-related emission studies mostly focuses on alternative fuels, emission reduction equipment, and energy efficiency works, this study reveals that even changes in air & seawater temperatures have the ability to affect ship exhaust emissions. Based on the findings, it appears feasible to reduce exhaust emissions in future research through the design or modification of ship systems that manipulate the temperature of the scavenge air. On the other side, this study utilized a one-year dataset of recorded seawater & air temperatures to conduct a simu-

lator-based investigation. Future research endeavors seek to effectively analyze additional data to conduct a more comprehensive analysis. Moreover, similar applications are intended to be carried out in diversified regions characterized by intense maritime activities and higher annual seawater & air temperature differentials.

Nomenclature

\dot{m}_f	Fuel Mass Flow
H_l	Fuel Lower Heating Value
V_o	Engine Cylinder Operating Volume
P_c	Compression Pressure
P_e	Mean Effective Pressure
P_z	Maximum Combustion Pressure
η_e	Engine Effective Efficiency
η_i	Indicated Efficiency
η_m	Mechanical Efficiency
D	Cylinder Bore
DNV	Det Norske Veritas
ERS	Engine Room Simulator
FO	Fuel Oil
IEC	International Electrotechnical Commission
IMO	International Maritime Organization
LO	Lubrication Oil
ME	Main Engine
n	Measured Revolution Speed
P_e	Measured Effective Power
P_i	Measured Power
P_{ml}	Power of Mechanical Losses
r/min	Revolution Per Minute
s	Cylinder Stroke
SFC_e	Specific Effective Fuel Consumption
SFC	Specific Fuel Consumption
STCW	Standard of Training Certification and Watchkeeping
SW	Seawater
z	Number of Engine Cylinders
τ	Engine Stroke
Φ_{ign}	Ignition Angle
Φ_{pz}	Timing Angle

Competing interest The author has no competing interests to declare that are relevant to the content of this article.

References

- Arslan O, Turan O (2009) Analytical investigation of marine casualties at the Strait of Istanbul with SWOT–AHP method. *Maritime Policy & Management*, 36(2): 131-145. <https://doi.org/10.1080/03088830902868081>
- Ay C, Seyhan A, Beşikçi EB (2022) Quantifying ship-borne emissions in Istanbul Strait with bottom-up and machine-learning approaches. *Ocean Engineering*, 258, 111864. <https://doi.org/10.1016/j.oceaneng.2022.111864>
- Banugopan VN, Prabhakar S, Annamalai K, Jayaraj S, Sentilkumar (2010) Experimental investigation on DI diesel engine fuelled by ethanol diesel blend with varying inlet air temperature. In *IEEE Frontiers in Automobile and Mechanical Engineering*, 128-134. <https://doi.org/10.1109/FAME.2010.5714809>
- Bilgili L, Buğra Çelebi U (2021) Estimation of ship flue gas emissions in dynamic operational conditions with ANN. *Proceedings of the Institution of Mechanical Engineers, Part M: Journal of Engineering for the Maritime Environment*, 235(2): 432-447. <https://doi.org/10.1177/1475090220979457>
- Buhaug Ø, Corbett J, Endresen Ø, Eyring V, Faber J, Hanayama S, Yoshida K (2009) Second IMO GHG Study 2009
- Ceylan BO (2023) Marine diesel engine turbocharger fouling phenomenon risk assessment application by using fuzzy FMEA method. *Proceedings of the Institution of Mechanical Engineers, Part M: Journal of Engineering for the Maritime Environment*, 14750902231208848. <https://doi.org/10.1177/14750902231208848>
- Ceylan BO, Akyuz E, Arslan O (2021) Systems-Theoretic Accident Model and Processes (STAMP) approach to analyse socio-technical systems of ship collision in narrow waters. *Ocean Engineering*, 239, 109804. <https://doi.org/10.1016/j.oceaneng.2021.109804>
- Ceylan BO, Akyuz E, Arslanoğlu Y (2022a) Modified quantitative systems theoretic accident model and processes (STAMP) analysis: A catastrophic ship engine failure case. *Ocean Engineering*, 253, 111187. <https://doi.org/10.1016/j.oceaneng.2022.111187>
- Ceylan BO, Karatuğ Ç, Arslanoğlu Y (2022b) A novel methodology for the use of engine simulators as a tool in academic studies. *Journal of Marine Science and Technology*, 1-13. <https://doi.org/10.1007/s00773-022-00902-9>
- Chybowski L, Gawdzińska K, Ślesicki O, Patejuk K, Nowosad G (2015) An engine room simulator as an educational tool for marine engineers relating to explosion and fire prevention of marine diesel engines. *Zeszyty Naukowe Akademii Morskiej w Szczecinie*
- Chybowski L, Strojcecki S, Markiewicz W (2020) Simulation-based training in fire prevention and fire-fighting of scavenge air receivers fires. *System Safety: Human-Technical Facility-Environment*, 2(1). <https://doi.org/10.2478/czoto-2020-0013>
- Dere C, Deniz C (2019) Load optimization of central cooling system pumps of a container ship for the slow steaming conditions to enhance the energy efficiency. *Journal of Cleaner Production*, 222, 206-217. <https://doi.org/10.1016/j.jclepro.2019.03.030>
- Dimitrios G (2012) Engine control simulator as a tool for preventive maintenance. *Journal of Maritime Research*, 9(1): 39-44
- Gaspar HM, Balland O, Aspen DM, Ross AM, Erikstad SO (2015) Assessing air emissions for uncertain life-cycle scenarios via responsive systems comparison method. *Proceedings of the Institution of Mechanical Engineers, Part M: Journal of Engineering for the Maritime Environment*, 229(4): 350-364. <https://doi.org/10.1177/1475090214522218>
- Google Earth, 2022. Marmara Region. <https://earth.google.com/web/@39.65101774,32.4124102,1085.39192015a,2091969.59857732d,35y,0h,0t,0r>. (Accessed 04 February 2023)
- Guo ZW, Yuan CQ, Bai XQ, Yan XP (2018) Experimental study on wear performance and oil film characteristics of surface textured cylinder liner in marine diesel engine. *Chinese Journal of Mechanical Engineering*, 31(1): 1-10. <https://doi.org/10.1186/s10033-018-0252-3>

- ISO (2022) ISO 3046-1: 2002- Reciprocating internal combustion engines—Performance—Part 1. <https://www.iso.org/standard/28330.html>. (Accessed 07 January 2023)
- Kanberoğlu B, Turan E, Kökkülünk G (2023) Decarbonization of Maritime Transportation: A Case Study for Turkish Ship Fleet. *Journal of Marine Science and Application*, 1-12. <https://doi.org/10.1007/s11804-023-00370-6>
- Kaptan M, Sivri N, Blettler MC, Uğurlu Ö (2020) Potential threat of plastic waste during the navigation of ships through the Turkish straits. *Environmental Monitoring and Assessment*, 192(8): 508. <https://doi.org/10.1007/s10661-020-08474-0>
- Karatağ Ç, Tadros M, Ventura M, Soares CG (2023) Strategy for ship energy efficiency based on optimization model and data-driven approach. *Ocean Engineering*, 279, 114397. <https://doi.org/10.1016/j.oceaneng.2023.114397>
- Knežević V, Orović J, Stazić L, Čulin J (2020) Fault tree analysis and failure diagnosis of marine diesel engine turbocharger system. *Journal of Marine Science and Engineering*, 8(12): 1004. <https://doi.org/10.3390/jmse8121004>
- Kocak G, Durmusoglu Y (2018) Energy efficiency analysis of a ship's central cooling system using variable speed pump. *Journal of Marine Engineering & Technology*, 17(1): 43-51. <https://doi.org/10.1080/20464177.2017.1283192>
- Kökkülünk G, Parlak A, Erdem HH (2016) Determination of performance degradation of a marine diesel engine by using curve based approach. *Applied Thermal Engineering*, 108: 1136-1146. <https://doi.org/10.1016/j.applthermaleng.2016.08.019>
- Kongsberg Maritime (2022) K-Sim® Engine-Engine Room Simulator. <https://www.kongsberg.com/digital/models-and-examples/k-sim-engine-models/sulzer-rta-container-vessel> (Accessed 19 January 2023)
- Kumar KS, Raj RTK (2013) Effect of fuel injection timing and elevated intake air temperature on the combustion and emission characteristics of dual fuel operated diesel engine. *Procedia Engineering*, 64: 1191-1198. <https://doi.org/10.1016/j.proeng.2013.09.198>
- Lamas MI, Rodríguez CG, Rodríguez JD, Telmo J (2013) Internal modifications to reduce pollutant emissions from marine engines. A numerical approach. *International Journal of Naval Architecture and Ocean Engineering*, 5(4): 493-501. <https://doi.org/10.2478/IJNAOE-2013-0148>
- Llomas X, Eriksson L (2019) Control-oriented modeling of two-stroke diesel engines with exhaust gas recirculation for marine applications. *Proceedings of the Institution of Mechanical Engineers, Part M: Journal of Engineering for the Maritime Environment*, 233(2): 551-574. <https://doi.org/10.1177/1475090218768992>
- MAN (2023) MAN B&W S60MC-C8.2-TII Project Guide. https://man-es.com/applications/projectguides/2stroke/content/epub/S60MC-C8_2.pdf (Accessed 15 August 2023)
- MGM (2022a) Monthly Temperature Analysis. <https://mgm.gov.tr/veridegerlendirme/sicaklik-analizi.aspx?s=a#sfB>. (Accessed 04 November 2022)
- MGM (2022b) Marmara Sea Sea Water Temperature. <https://www.mgm.gov.tr/FILES/resmi-istatistikler/denizSuyu/Marmara-Deniz-Suyu-Sicakligi-Analizi-2021.pdf>. (Accessed 04 November 2022)
- Mocerino L, Soares CG, Rizzuto E, Balsamo F, Quaranta F (2021) Validation of an emission model for a marine diesel engine with data from sea operations. *Journal of Marine Science and Application*, 20(3): 534-545. <https://doi.org/10.1007/s11804-021-00227-w>
- Monieta J (2021) Diagnosing marine piston engines driving generators at different operational loads. *Journal of Marine Science and Engineering*, 9(2): 132. <https://doi.org/10.3390/jmse9020132>
- Mrzljak V, Žarković B, Prpić-Oršić J (2017) Marine slow speed two-stroke diesel engine-numerical analysis of efficiencies and important operating parameters. *Machines Technologies Materials*, 11(10): 481-484
- Nahim HM, Younes R, Nohra C, Ouladsine M (2015) Complete modeling for systems of a marine diesel engine. *Journal of Marine Science and Application*, 14: 93-104. <https://doi.org/10.1007/s11804-015-1285-y>
- Ni P, Wang X, Li H (2020) A review on regulations, current status, effects and reduction strategies of emissions for marine diesel engines. *Fuel*, 279: 118477. <https://doi.org/10.1016/j.fuel.2020.118477>
- Noor CM, Noor MM, Mamat R (2018) Biodiesel as alternative fuel for marine diesel engine applications: A review. *Renewable And Sustainable Energy Reviews*, 94: 127-142. <https://doi.org/10.1016/j.rser.2018.05.031>
- Pan W, Yao C, Han G, Wei H, Wang Q (2015) The impact of intake air temperature on performance and exhaust emissions of a diesel methanol dual fuel engine. *Fuel*, 162: 101-110. <https://doi.org/10.1016/j.fuel.2015.08.073>
- Ramsay W, Fridell E, Michan M (2023) Maritime energy transition: future fuels and future emissions. *Journal of Marine Science and Application*, 22. <https://doi.org/10.1007/s11804-023-00369-z>
- Ryu Y, Lee Y, Nam J (2016) Performance and emission characteristics of additives-enhanced heavy fuel oil in large two-stroke marine diesel engine. *Fuel*, 182: 850-856. <https://doi.org/10.1016/j.fuel.2016.06.029>
- Sarjovaara T, Larimi M, Vuorinen V (2015) Effect of charge air temperature on E85 dual-fuel diesel combustion. *Fuel*, 153: 6-12. <https://doi.org/10.1016/j.fuel.2015.02.096>
- Stanivuk T, Lalić B, Žanić Mikuličić J, Šundov M (2021) Simulation modelling of marine diesel engine cooling system. *Transactions on Maritime Science*, 10(1): 112-125. <https://doi.org/10.7225/toms.v10.n01.008>
- Tadros M, Ventura M, Guedes Soares C (2020) Optimization of the performance of marine diesel engines to minimize the formation of SOx emissions. *Journal of Marine Science and Application*, 19, 473-484. <https://doi.org/10.1007/s11804-020-00156-0>
- Tadros M, Ventura M, Soares CG (2023) Review of current regulations, available technologies, and future trends in the green shipping industry. *Ocean Engineering*, 280: 114670. <https://doi.org/10.1016/j.oceaneng.2023.114670>
- Tonoğlu F, Atalar F, Başkan İB, Yıldız S, Uğurlu Ö, Wang J (2022) A new hybrid approach for determining sector-specific risk factors in Turkish Straits: Fuzzy AHP-PRAT technique. *Ocean Engineering*, 253, 111280. <https://doi.org/10.1016/j.oceaneng.2022.111280>
- Torregrosa AJ, Olmeda P, Martin J, Degraeuwe B (2006) Experiments on the influence of inlet charge and coolant temperature on performance and emissions of a DI Diesel engine. *Experimental Thermal and Fluid Science*, 30(7): 633-641. <https://doi.org/10.1016/j.expthermflusci.2006.01.002>
- Toscano D, Murena F, Quaranta F, Mocerino L (2021) Assessment of the impact of ship emissions on air quality based on a complete annual emission inventory using AIS data for the port of Naples. *Ocean Engineering*, 232: 109166. <https://doi.org/10.1016/j.oceaneng.2021.109166>
- Vera-García F, Pagán Rubio JA, Hernández Grau J, Albaladejo Hernández D (2019) Improvements of a failure database for marine diesel engines using the RCM and simulations. *Energies*, 13(1): 104. <https://doi.org/10.3390/en13010104>

- Wang H, Zhou P, Wang Z (2017) Reviews on current carbon emission reduction technologies and projects and their feasibilities on ships. *Journal of Marine Science and Application*, 16: 129-136. <https://doi.org/10.1007/s11804-017-1413-y>
- Wärtsilä-Transas (2023) ERS 5000 Engine Room Simulator. <https://www.transas.com/products/simulation/engine-room-and-cargo-handling-simulators/ERS-5000>. (Accessed 19 January 2023)
- Welaya YM, Mosleh M, Ammar NR (2013) Thermodynamic analysis of a combined gas turbine power plant with a solid oxide fuel cell for marine applications. *International Journal of Naval Architecture and Ocean Engineering*, 5(4): 529-545. <https://doi.org/10.2478/IJNAOE-2013-0151>
- Woo C, Kook S, Hawkes ER (2016) Effect of intake air temperature and common-rail pressure on ethanol combustion in a single-cylinder light-duty diesel engine. *Fuel*, 180: 9-19. <https://doi.org/10.1016/j.fuel.2016.04.005>
- Wu HW, Hsu TT, He JY, Fan CM (2017) Optimal performance and emissions of diesel/hydrogen-rich gas engine varying intake air temperature and EGR ratio. *Applied Thermal Engineering*, 124: 381-392. <https://doi.org/10.1016/j.applthermaleng.2017.06.026>
- Yang R, Theotokatos G, Vassalos D (2020) Parametric investigation of a large two-stroke marine high-pressure direct injection engine by using computational fluid dynamics method. *Proceedings of the Institution of Mechanical Engineers, Part M: Journal of Engineering for the Maritime Environment*, 234(3): 699-711. <https://doi.org/10.1177/1475090219895639>
- Yuksel O, Bayraktar M, Sokukcu M (2023) Comparative study of machine learning techniques to predict fuel consumption of a marine diesel engine. *Ocean Engineering*, 286: 115505. <https://doi.org/10.1016/j.oceaneng.2023.115505>
- Yutuc W (2020) An investigation on the overall efficiency of a ship with shaft generator using an engine room simulator. In *Advancement in Emerging Technologies and Engineering Applications*, 255-265. Springer, Singapore
- Zetterdahl M, Salo K, Fridell E, Sjöblom J (2017) Impact of aromatic concentration in marine fuels on particle emissions. *J. Mar. Sci. App*, 16(3): 352-361
- Zincir BA, Arslanoglu Y (2024) Comparative life cycle assessment of alternative marine fuels. *Fuel*, 358: 129995. <https://doi.org/10.1016/j.fuel.2023.129995>